

Supporting Online Material for

Enhanced Enantioselectivity in Excitation of Chiral Molecules by Superchiral Light

Yiqiao Tang and Adam E. Cohen*

*To whom correspondence should be addressed. E-mail: cohen@chemistry.harvard.edu

Published 15 April 2011, *Science* **332**, 333 (2011)
DOI: 10.1126/science.1202817

This PDF file includes:

Materials and Methods
Figs. S1 to S4
References and Notes

Supporting Online Material for

Enhanced enantioselectivity in excitation of chiral molecules by superchiral light

Yiqiao Tang¹

Adam E. Cohen^{1,2*}

¹ Department of Physics

² Department of Chemistry and Chemical Biology, Harvard University, 12 Oxford Street, Cambridge, MA 02138

* cohen@chemistry.harvard.edu

Chiral fluorophores

Figure S1(a) shows the molecular structures of the fluorophores used in this experiment. The chiral fluorophores were the two enantiomers of a binaphthylene-perylenebiscarboxydiimide dimer, generously provided by Prof. Heinz Langhals.(S1) The achiral control was N,N'-bis(1-hexylheptyl)-perylene-3,4:9,10-bis-(dicarboximide) (16459-10MG-F, Sigma-Aldrich). Figure S1(b) shows the CD spectrum in toluene of both enantiomers taken on a CD spectrometer (J-710 JASCO). A strong peak in the CD at 540 nm coincided closely to our probing wavelength of 543.5 nm. The achiral perylene showed no detectable CD.

Sample preparation

The goal was to position a chiral film of thickness much less than the wavelength of light in a standing wave generated by reflection of CPL off an imperfect mirror. The film had to be positioned with extreme stability relative to the mirror so that drift of the interference fringes did not overwhelm the small changes in total fluorescence due to CD. The fractional changes in fluorescence in conventional CD are expected to be of order $\sim 10^{-3}$, implying that the separation of the film and the mirror had to be stable to $\lambda/10^4 \approx 0.5 \text{ \AA}$ during a 20-minute data acquisition. This goal was achieved by depositing the chiral film and the mirror on opposite sides of a 170 μm -thick glass coverslip.

Figure S2 shows the sample preparation. A box of #1.5 coverslips (VWR) was searched for coverslips that showed straight, well-spaced interference fringes when viewed under fluorescent room lights. A favorable coverslip was cleaned and coated on one side with 19 nm of Al via thermal evaporation. This mirror had a reflectivity of 72% at 543 nm. The Al-coated side of the coverslip was then bonded to a 1 mm thick glass slide using optical adhesive (Norland 68). The glass slide protected the Al film and provided a rigid support for the coverslip.

Chiral fluorophore ($2 \times 10^{-4} \text{ M}$) and poly(methyl methacrylate) (PMMA, molecular weight 350,000, 0.75%) were dissolved in toluene. A chiral film was deposited by spin coating the solution onto the exposed face of the coverslip (60 s at 2800 rpm). The film thickness was determined to be 10 nm by ellipsometry. We then covered half of the film with a piece of polydimethylsiloxane (PDMS), which served as an etch mask for the next step. The exposed film was removed in a plasma etcher (500 mTorr, 5 min. SPI Plasma Prep II), while the part covered by the PDMS remained on the coverslip.

Leaving the PDMS over the chiral film, we spin coated a solution of the achiral control ($2 \times 10^{-4} \text{ M}$ with 0.75% PMMA in toluene, 60 s at 2800 rpm) onto the exposed part of the

coverslip. We then masked the achiral region with a second piece of PDMS, leaving a thin gap between the two pieces of PDMS. This assembly was subjected to a second round of plasma etching, to remove a thin trench of polymer separating the chiral and achiral regions. The PDMS masks were then removed. A second sample was prepared as above, using the opposite enantiomer. This procedure led to two samples in which achiral and chiral thin layers each occupied half of the coverslip, with a small gap in between.

Samples for fluorescence detected circular dichroism (FDCD) imaging using conventional circularly polarized light were made as above, with the omission of the Al evaporation step. Figure S3(a) shows a fluorescence image of a sample without the Al mirror. The achiral region is on the top and the chiral region on the bottom. The horizontal dark stripe is the gap between the films. Figure S3(b) is a fluorescence image of a sample with the mirror. The arrangement is the same as in Fig. S3(a), with the addition of the vertical stripe due to the interference of incident and reflected light.

Experimental layout

The optical setup is shown in Figure S3(c). This system was designed to be immune to laser pointing instability and intensity fluctuations, while permitting measurements of fluorescence intensity under well-defined polarization conditions to a fractional precision of 4×10^{-5} .

The light source was a HeNe laser operating at 543.5 nm (JDS1674P, power: 0.9 mW). A narrow-band excitation filter (Z543/10X Chroma) removed plasma emission at other wavelengths. The beam was coupled through a single mode optical fiber to eliminate pointing instability. The beam was then expanded to a diameter of 7.8 mm and polarized by a Glan-laser polarizer (GL10-A Thorlabs). The principal axis of linear polarization was chosen to be vertical, to minimize distortion of the polarization upon reflection on the dichroic mirror (Z543RDC Chroma). After the dichroic, the light passed through a liquid crystal variable retarder (LCVR, LRC - 200 - VIS, Meadowlark Optics). The LCVR was driven with a 2 kHz square wave with amplitude selected to generate the desired circular polarization incident on the sample. The LCVR was mounted on a linear motion stage (MT1-Z8 Thorlabs) which could translate the LCVR perpendicular to the beam. During each acquisition the LCVR was slowly translated side to side. This motion was essential to average out subtle interference fringes due to imperfections in the LCVR that otherwise contaminated the data analysis.

The sample was aligned perpendicular to the beam, with illumination falling equally on the chiral and achiral regions. Fluorescence passed back through the LCVR and the dichroic mirror. An emission filter (HQ565lp Chroma) passed fluorescence while blocking scattered laser light. A Nikon macro-lens (60 mm f/2.8D AF Micro-Nikkor) imaged fluorescence from the sample onto an Andor iXon+ electron-multiplying CCD (DU-897E-CS0-UVB), cooled to -70 °C.

Imaging of Fluorescence Detected Circular Dichroism

A program written in LabView synchronized acquisition of images with application of voltages to the LCVR. The LCVR had a 30 ms response time to a change in the amplitude of its driving voltage, so we waited 100 ms between changing the retardance and acquiring an image. Full field images (512 x 512 pixels) were acquired with an exposure time of 0.8 s and an electron-multiplying gain of 5. For each sample, 400 images were acquired with a switch in the chirality of CPL between each frame. Every 40 frames the lateral position of the LCVR was shifted by 0.2 mm using the motorized translation stage.

The LCVR and glass produced autofluorescence that led to a spatially inhomogeneous background signal. To correct for this autofluorescence, we prepared a sample lacking fluorophores and repeated the experiment, acquiring another 400-images alternately under left- and right-CPL. We averaged the left-CPL and right-CPL background images separately. Each average image was subtracted from the images with a fluorescent film taken under corresponding helicity of the illumination.(S2)

For each image frame, we normalized the image by the total intensity of the achiral region. This procedure eliminated noise due to fluctuations in the intensity of the laser or the sensitivity of the camera. We calculated a map of the dissymmetry factor by

$$g_{image} = 2 \frac{(F_L - F_R)}{(F_L + F_R)},$$

where F_L and F_R are the normalized images under left- and right-CPL illumination, averaging over the complete dataset.

Figure S4 shows the FDCD measurement on chiral thin films without superchiral enhancement. The maps of the dissymmetry factor show the p-enantiomer as having a positive dissymmetry factor (brighter than the control) and the m-enantiomer as having a negative dissymmetry factor (darker than the control).

Predicted superchiral enhancement

The predicted dissymmetry factor as a function of position in a superchiral standing wave is:(S3)

$$\frac{g}{g_{CPL}} = \frac{1 - R}{1 + R - 2\sqrt{R} \cos(2kz)}, \quad [S1]$$

where R is the reflectivity of the mirror used to generate the standing wave and k is the wavevector of the light. To fit this formula to our data, the value of kz at each position is determined by the fringe spacing in the interference pattern. Eq. S1 is plotted as the black line in Fig. 3 in the main text.

At the superchiral nodes, Eq. S1 predicts that the maximum enhancement in CD is:

$$g = g_{CPL} \frac{1 + \sqrt{R}}{1 - \sqrt{R}}.$$

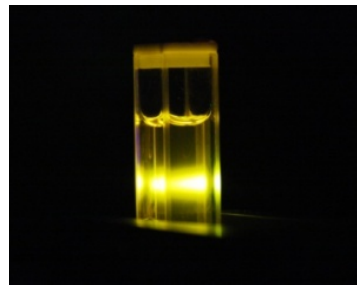
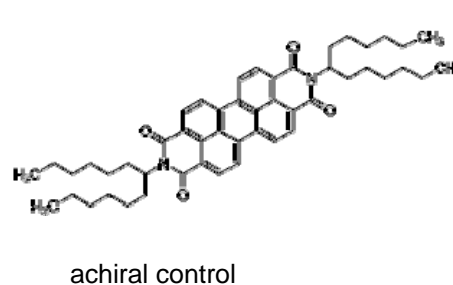
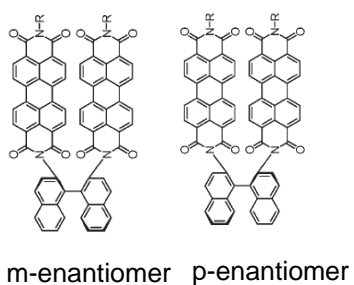
The electric energy density at the node, which determines the total fluorescence brightness, is:

$$U_e = U_{e,CPL} (1 - \sqrt{R})^2,$$

where $U_{e,CPL}$ is the electric component of the energy density of the incident circularly polarized plane wave. Higher reflectivity leads to larger chiral selectivity, but at the expense of a smaller electric energy density at the node, and hence a smaller overall fluorescence intensity at the node.

We chose a mirror thickness of 19 nm, which yielded a reflectivity of 72% at 543 nm. At the node, the theoretical enhancement was $g = 12.2 g_{CPL}$, while the electric energy density was $U_e = 0.023 U_{e,CPL}$. This choice of parameters was a compromise between achieving a large enhancement in the chiral asymmetry and a reasonable photon flux from the sample.

(A)



(B)

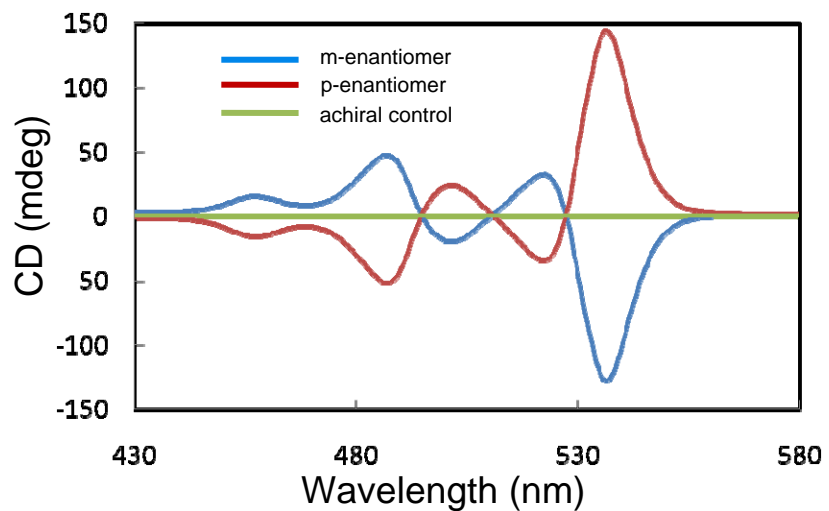


Figure S1. Chiral fluorophores. (A) Binaphthyl perylene dimer. R = 1-hexylheptyl group. An achiral perylene derivative was used as a control. Right: photograph of a solution of the achiral perylene in toluene under excitation at 543.5 nm. (B) CD spectra of the chiral fluorophores and achiral control.

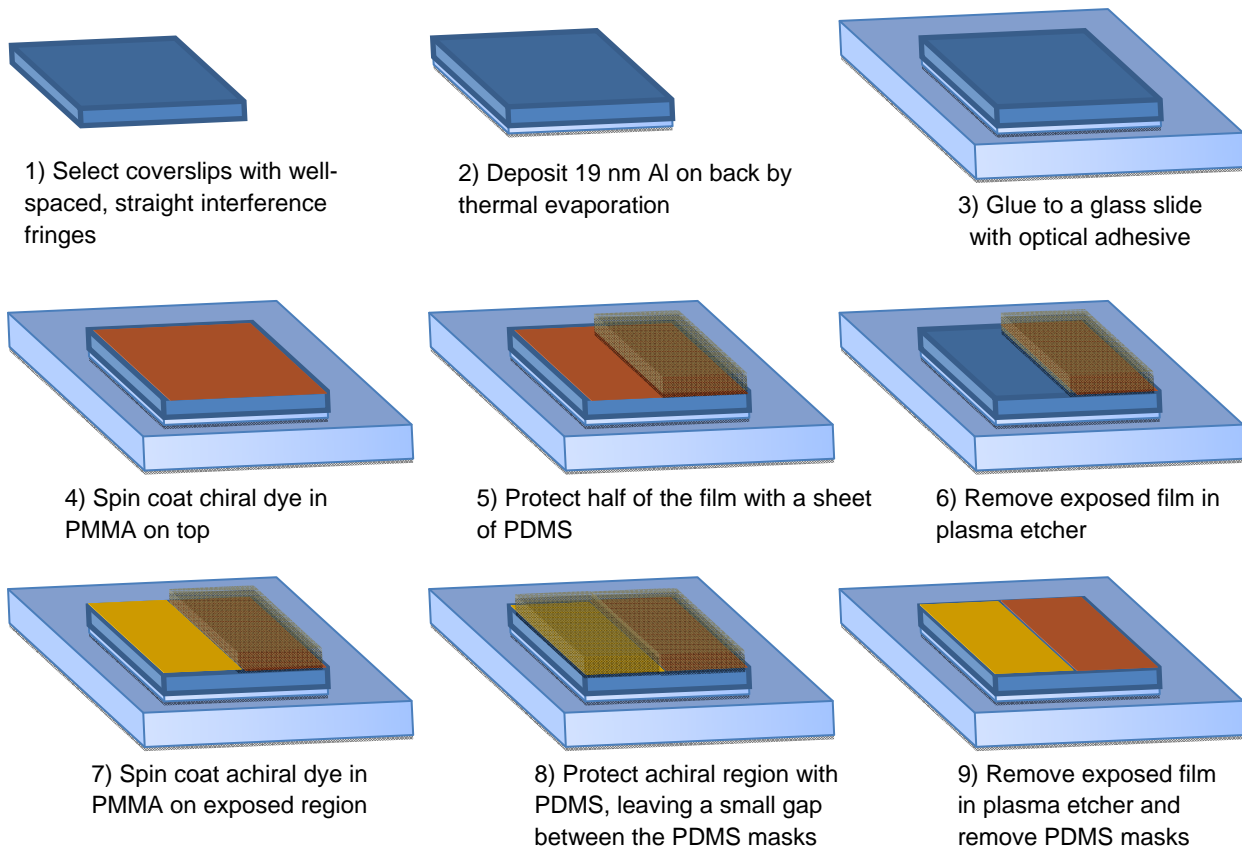


Figure S2. Procedure for sample preparation. Control samples for conventional thin-film CD measurements were fabricated as above, starting at step 3.

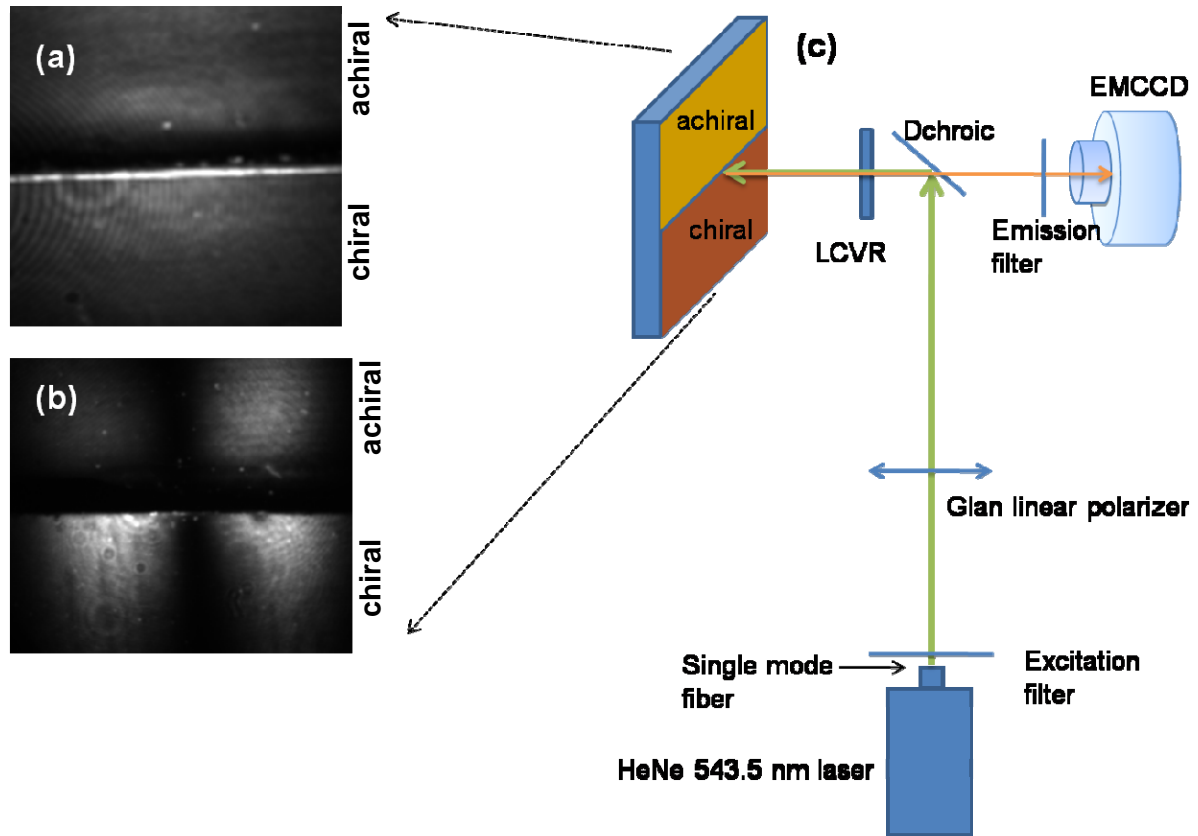


Figure S3. Experimental apparatus. (a) Photograph of fluorescent sample without Al mirror. (b) Photograph of fluorescent sample with Al mirror and a vertical interference stripe. (c) Experimental layout.

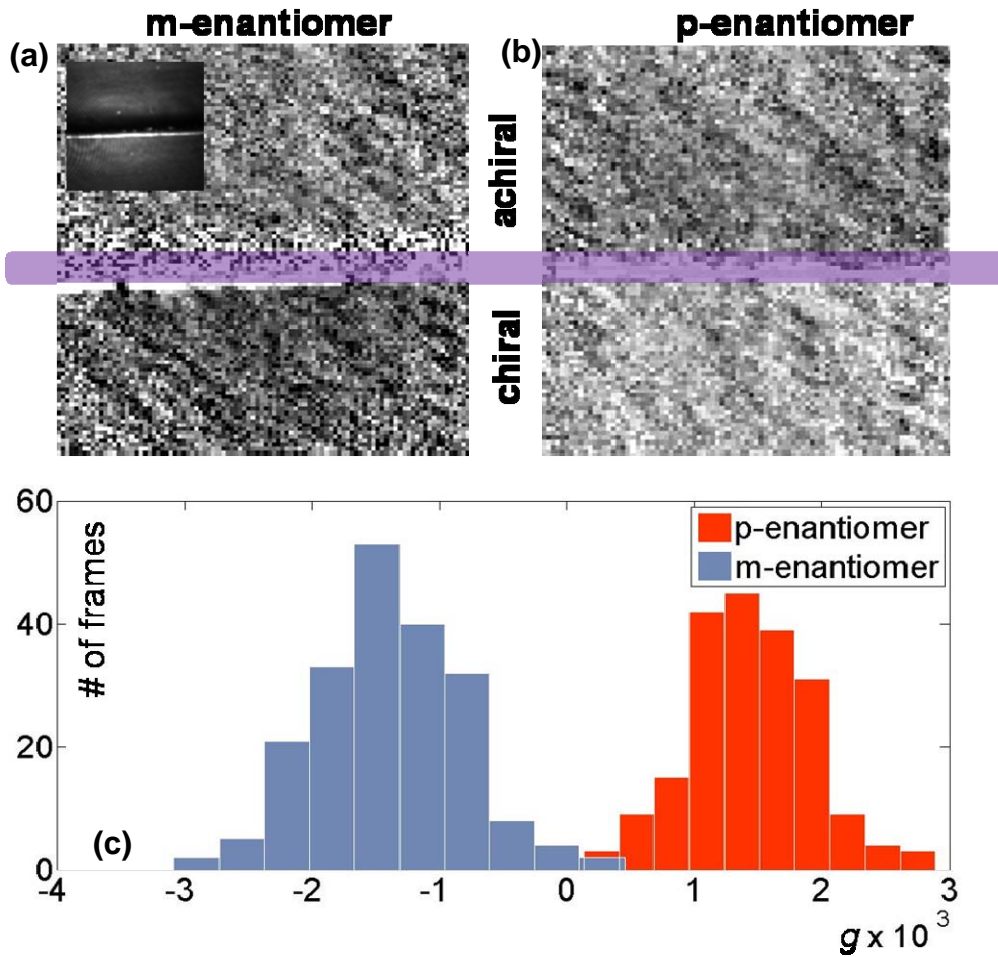


Figure S4. Fluorescence detected circular dichroism on thin films without superchiral enhancement. (a) Map of dissymmetry factor for the m-enantiomer and achiral control. Inset: photo of the fluorescent sample. (b) Map of dissymmetry factor for the p-enantiomer and achiral control. (c) Histogram of dissymmetry factor based on 400 images (for both the m- and p-enantiomer)

References

S1. H. Langhals, J. Gold, *Liebigs Ann* **1997**, 1151 (1997).

S2. Due to the difference between the background autofluorescence of the LCVR under R- and L-CPL, a scaling factor F was applied to the two averaged background images in the subtraction. To generate figure S4, we chose $F = 1$ for R-CPL and $F = 1.013$ for L-CPL; to generate Figure

3(B) in the main text, we chose $F = 1$ for R-CPL (for both enantiomers), $F = 1.008$ for m-enantiomer under L-CPL , and $F = 1.012$ for p-enantiomer under L-CPL.

S3. Y. Tang, A. E. Cohen, *Phys. Rev. Lett.* **104**, 163901 (2010).